Japanese Journal of Applied Physics **54**, 06GA02 (2015) **REGULAR PAPER**
http://dx.doi.org/10.7567/JJAP.54.06GA02

Calculated photoionization cross sections using Quantemol-N

Will J. Brigg[1,2], Alex G. Harvey[3], Anna Dzarasova[2*], Sebastian Mohr[2], Danilo S. Brambila[3], Felipe Morales[3], Olga Smirnova[3], and Jonathan Tennyson[1]

[1]*Department of Physics and Astronomy, University College London, London WC1E 6BT, U.K.*
[2]*Quantemol Ltd., University College London, London WC1E 6BT, U.K.*
[3]*Max Born Institute, 12489 Berlin, Germany*
E-mail: anna@quantemol.com

Received December 8, 2014; accepted March 17, 2015; published online May 11, 2015

Quantemol-N is an expert system designed to run the widely used UK Molecular R-matrix code (UKRMol). Originally designed to consider electron–molecule collision problems, here we present an extension to treat molecular photoionization. Sample results are given for the photoionization of molecular nitrogen and methane. Comparisons are made with experimental results showing good agreement.

1. Introduction

The removal of an electron from an atom or molecule by the action of light, photoionization, is an important process in a wide range of natural phenomena. It can, for example, be the plasma initiator in a number of environments or it can play a key role in the radiative transport and ionization balance within plasmas.

Models of photoionizing plasmas require accurate cross sections for the species in the plasma. While these are generally available from laboratory experiments for stable molecules, such cross sections are hard to measure for the radicals and ions which form many of the species that make up a typical molecular plasma.

Quantemol-N[1)] provides an expert system for running the UK Molecular R-matrix codes, UKRMol.[2)] These codes provide a state-of-the-art general computer package for considering low-energy electron–molecule collisions based on the use of R-matrix theory.[3,4)] Quantemol-N makes these codes easy to use and provides a number of extra features, useful for plasma models, such as an extension to higher electron-collision energies and the estimation of dissociative attachment cross sections.[5)]

The diatomic implementation of the UK molecular R-matrix codes[6)] was adapted some time ago for the study of photoionization.[7–9)] However this adaptation was not included in the development of either the UK[10)] or Bonn[11)] polyatomic R-matrix codes. Subsequently both Hiyama and Kosugi[12)] and Tashiro[13)] developed implementations of photoionization based on the R-matrix method which have been successfully used to study X-ray photoionization.[14,15)] Recently Harvey and co-workers[16)] have adapted the current UKRMol codes to treat photoionization, allowing for the calculation of observables resolvable in the final state of the resultant ion, the photon polarisation and energy, the molecular orientation, and the electron emission direction. This work required considerable new technical developments[17)] because of the use of an efficient but non-standard formalism to generate the wave functions in the modern implementation of the codes.[18)] Here we build on the work of Harvey et al. to provide Quantemol-N with the capability to calculate photoionization observables.

There are a number of other theoretical procedures available for calculating near-threshold photoionization cross sections. These methods include use of single-centre expansions[19,20)] and time-dependent density functional theory (TDDFT),[21,22)] both of which struggle to account fully for Feshbach resonances.[23)] Closer in spirit to the R-matrix method used here are the complex Kohn variational method[24,25)] and the Schwinger variational method.[26–28)] Cross comparisons between the R-matrix, Kohn and Schwinger methods for both electron–molecule scattering[29–31)] and photoionization[32)] suggests that the methods give very similar results for the same model. The R-matrix method is particularly efficient for considering large numbers of energies which can be important for resolving structures due to resonances.

We present results for the photoionization of molecular nitrogen, N_2, and methane, CH_4. Nitrogen is a key component of the Earth's atmosphere and many plasmas. There are also several high quality experimental studies available[33,34)] against which we can compare. Methane is also a trace atmospheric species, and a common plasma component; again there are a number of good experimental studies of its photoionization cross section.[35,36)]

2. Method

The formalism for treating photoionization within the R-matrix method was originally presented by Burke and Taylor[37)] for atoms. This formalism was extended by Burke for molecules.[38)] The recent implementation builds on this formalism but takes advantage of a number of constructs to accelerate the calculations; the reader is referred to the papers of Harvey et al.[16)] for more details.

The photoionization cross sections are computed within the length gauge and are given by[7,16)]

$$\frac{d\sigma_{if}}{d\boldsymbol{k}_f} = 4\pi^2 \alpha a_0^2 \omega |\boldsymbol{d}_{if}(\boldsymbol{k}_f) \cdot \hat{\boldsymbol{\epsilon}}|^2 \quad (1)$$

where α is the fine structure constant, a_0 is the Bohr radius, ω the photon energy in atomic units, and $\hat{\boldsymbol{\epsilon}}$ is the polarisation direction of the incident photon in the molecular frame. $\boldsymbol{d}_{if}(\boldsymbol{k}_f)$ is the molecular frame transition dipole between the initial state, i, and a single continuum state, f, as a function of the ejected electron momentum, $\boldsymbol{k}_f$.

Although it is possible to construct bound state wavefunctions using negative-energy scattering calculations,[39)] this is not generally necessary as the target wavefunction is usually confined to lie within the R-matrix sphere. In this case the integral in Eq. (1) can be restricted to the inner

region, and both the initial and final state can be expanded in terms of their inner-region, energy-independent solutions, $\psi_k^{(N)}$. One can expand both the energy-dependent continuum

$$\Psi_{fk_f}^{(-)} = \sum_k A_{fk}(\boldsymbol{k}_f)\psi_k^{(N)} \tag{2}$$

and bound state

$$\Phi_i^N = \sum_k B_{ik}\psi_k^{(N)}. \tag{3}$$

wave functions in terms of these inner-region solutions. Substituting these into Eq. (1), we obtain

$$\boldsymbol{d}_{if}(\boldsymbol{k}_f) = \sum_{kk'} A_{fk}^*(\boldsymbol{k}_f)\langle\psi_k^{(N)}|\boldsymbol{d}|\psi_{k'}^{(N)}\rangle B_{ik'} \tag{4}$$

which give the dipole in terms of $A_{fk}^*(\boldsymbol{k}_f)$, $B_{ik'}$, and the dipole transition moments, $\langle\psi_k^{(N)}|\boldsymbol{d}|\psi_{k'}^{(N)}\rangle$, between inner-region solutions.

Within the UK R-matrix codes,[2] quantities are obtained by by performing a scattering calculation on the ion the initial target is ionised into, with the additional use of a heavily modified version of the module denprop, called cDenprop, which produces the dipoles between inner region solutions; compAk, a new outer region subroutine for determining continuum wavefunctions, and a new program DipElm[16] which computes the final cross sections.

These modules have been incorporated into Quantemol-N, vastly reducing the difficulty of performing calculations. Despite this, however, photoionization cross sections can be harder to converge than electron scattering calculations. In particular they often display slower convergence with respect to the number of orbitals included in the active space and the number of states included in the close coupling expansion. In part this is due to the need to use a common set of orbitals to represent both the target molecule and the photoionized ion. A partial solution to this problem is to simply use better orbitals, such as those generated by either a multi-reference self-consistent field (MCSCF) calculation or (pseudo) natural orbitals arising from a multireference configuration (MRCI) calculation. We use the quantum chemistry package MOLPRO[40] to provide the orbitals in these cases. It is possible to input MOLPRO orbitals directly into Quantemol-N. Another approach, used by Lebach et al.,[41] is to use the same SCF orbitals for the photoionized ion, and then augment these with virtual orbitals from an ion state-averaged MCSCF for the weakly occupied virtual orbitals. This approach works best when only photoionization to the ground state of the ion is considered.

The Quantemol-N photoionization module is heavily based on the original electron-scattering implementation,[1] with a few straightforward changes such as the calculations are based on photon energies instead of electron collision energies. The new Quantemol-N code (version 4.6) is actually capable of considering photoionization from oriented molecules. However the results presented below are all for the more usual situation of randomly-oriented molecules, as this situation is more important for plasma models.

3. Calculations

N_2 was considered at its equilibrium bondlength of $1.125\,a_0$. The nitrogen photoionized ion was represented using a cc-pVTZ Gaussian Type Orbital (GTO) basis set and complete active space configuration interaction (CAS-CI) treatment[42] which involved placing the highest 10 electrons in 7 orbitals (when spatial degeneracy is taken into account). This gives a CAS which can be described by

$$[1\sigma_g, 2\sigma_g, 1\sigma_u, 2\sigma_u]^4[3\sigma_g, 4\sigma_g, 3\sigma_u, 1\pi_g, 1\pi_u]^{10}.$$

Unusually, for N_2, the SCF orbitals proved sufficient to obtain well-converged calculations. This is probably because the SCF orbitals for N_2 and N_2^+ are rather similar.

For methane, a bondlength of $1.098\,a_0$ and a 6-31G GTO basis set were used. The CAS-CI model employed placed 6 electrons in 8 orbitals, giving a CAS of $[1a, 2a]^4[3a, 1t_2, 2t_2]^6$. The labelling of these orbitals in their T_d point group representation is not possible from the labelling given by the irreducible representations of the D_2 point group actually used to perform the calculation, so the correct labels were inferred from equivalent calculations done in C_{2v}. Another issue is that, in the case of methane, the ionic state is degenerate in Abelian point groups, which require state-averaged orbitals to ensure that the symmetry is not broken; this feature not yet implemented in Quantemol-N for SCF orbitals, so MOLPRO was used to provide state averaged CASSCF orbitals.

For both molecules, the continuum calculations used a set of s, p, d, g, f symmetry GTOs[43] placed at the molecular center-of-mass to represent the photoionized electron and an R-matrix sphere, which represents the inner region of the calculation, of $12\,a_0$. All states up to 30 eV (the first 105 states, and 46 states, respectively, for nitrogen and methane) generated from the initial CAS-CI calculations were included in the final close-coupling expansions. This allows both for convergence of the calculations and explicit inclusion of channels involving photoionization to excited states of the molecular ions.

Calculations were performed as a function of photon energy, with photon energies up to 30 eV above the ionisation thresholds being explicitly considered. For comparison purposes in both cases the photoionization threshold has been shifted to the empirical values. For N_2 a value 15.81 eV[44] was used. The computed, vertical value is 16.85 eV; about half the difference between the two values comes from nuclear relaxation effects. The remaining discrepency, which is in line with a recent much more sophisticated R-matrix study of bound and continuum states of this system,[45,46] can be attributed to incomplete valence correlation effects. Interestingly the Koopman's theorem vertical ionisation energy is 15.34 eV, which is closer to the experimental values. For methane the corresponding values are: experimental 12.61 eV,[47] R-matrix 14.18 eV and Koopman's 13.10 eV.

4. Results

Figure 1 presents our photoionization cross sections for N_2 and compares them with experiment. The agreement with the experimental results is generally good. Both theory and experiment show sharp features which are caused by quasi-bound states lying in the continuum, generally called resonances. Here our calculations show a resonance series appearing in the energy region spanning 0.5 eV above the photoionization threshold. Such resonances are a true feature

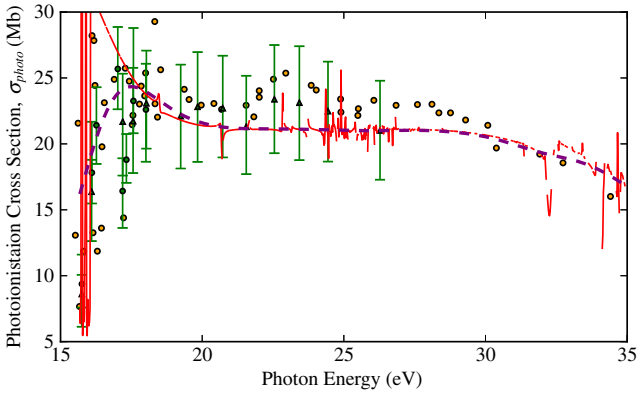

Fig. 1. (Color online) N_2 photoionization cross section, solid line, and Gaussian convolved cross section ($\sigma = 0.5$ eV), dashed line; and the experimental results: 5 cm ion chamber, with 10 Å^2 resolution (triangles); and 3 cm ion chamber, with 5 Å^2 resolution (filled circles) both from Wainfan et al.[34] Plus the experimental results of Samson et al.[33] (gray circles).

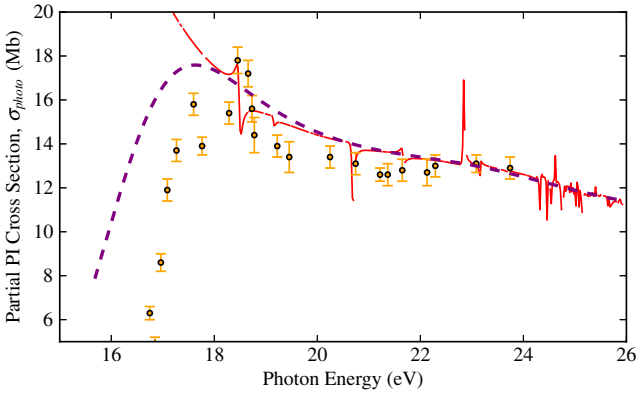

Fig. 3. (Color online) N_2 partial photoionization cross section to final ionic state A $^2\Pi_u^+$, solid line, and Gaussian convolved cross section ($\sigma = 0.5$ eV), dashed line; and theexperimental results of Samson et al.[33] (gray circles).

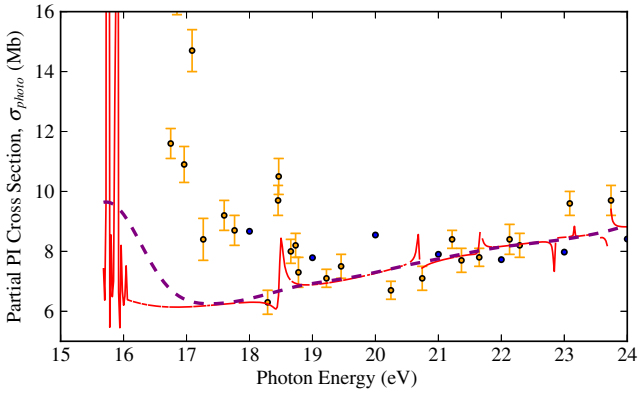

Fig. 2. (Color online) N_2 partial photoionization cross section to final ionic state X $^2\Sigma_g^+$, solid line, and Gaussian convolved cross section ($\sigma = 0.5$ eV), dashed line, compared with the experimental results of Samson et al.[33] (gray circles) and Hammett et al.[48] (black circles).

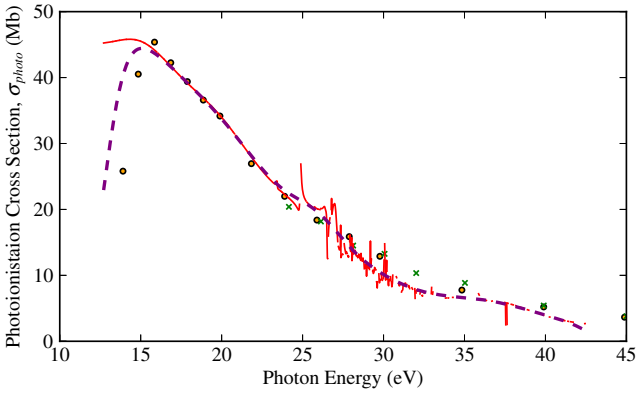

Fig. 4. (Color online) CH_4 partial photoionization cross section yielding a final ionic state of T_2 symmetry. This work: solid line, and Gaussian convolved cross section ($\sigma = 1$ eV), dashed line; for comparison the experimental results of Backx and Van der Wiel[35] (gray circles) and Van der Wiel et al.[36] (crosses) are also given.

of the photoionization process but are too sharp in the fixed-geometry calculations presented here because of the neglect of the vibrational motion of the molecule. To allow for this motion we use a Gaussian of width 0.5 eV to smooth out the resonances. A correct handling of the resonances is less important at higher energies since there fewer resonances. As the Gaussian smoothing is only approximate, agreement is less good in the near-threshold region.

Figures 2 and 3 show partial cross sections for photoionization leaving the ion in the ground and first excited state, respectively. Of the the two partial cross sections that give the major contribution to the total cross section, one overestimates, and the other under estimates, when compared with the experimental results,[33,34] especially in the low energy region below 18 eV. These differences cancel each other out when combined to give the total cross section: partial cross sections are sensitive to channel-coupling effects such as intensity borrowing from a stronger channel to a weaker channel, and it is possible that our model does not adequately describe the coupling at low energies. Another possibility could be that the deconvolution procedure of Samson et al.[33] is based on the use of slightly incorrect branching ratios, as the deconvolution of the experimental total cross section into the partial cross sections is far from straightforward.

Figure 4 shows our results for methane, and comparisons with experiment. A measured total cross section was not found in the literature, but photoionization to lowest T_2 ionic state partial cross section makes the only contribution to the total cross section until the next threshold at approximately 25 eV, above which this transition still contributes more than 90% of the cross sections. These partial cross sections, which leave the ion in an excited electronic states, were also studied experimentally by Backx and Van der Wiel[35] and Van der Weil et al.[36] These results, not shown here, are also accurately reproduced by Quantemol-N.

5. Conclusions

Photoionization has been implemented within the Quantemol-N expert system, simplifying the use of the UK molecular R-matrix codes in combination with the new photoionization routines. Calculations have been performed for a number of molecular targets, including N_2 and CH_4, results for which are presented here. The calculations are generally in good agreement with experimental measurements suggesting that the code should give good results for

systems not easily amenable to observation, such as radical species commonly found in molecular plasmas. The methodology can also consider angularly resolved cross sections and hence yield β parameters.

Acknowledgments

This work was performed as part of the CORINF EU network (Grant No. ITN-2010-264951). Funding from the UK Science and Technology Facilities Council (STFC), Einstein Foundation project A-211-55 Attosecond Electron Dynamics and ERA-Chemistry project PIM2010EEC-00751 is also gratefully acknowledged.

1) J. Tennyson, D. B. Brown, J. J. Munro, I. Rozum, H. N. Varambhia, and N. Vinci, J. Phys.: Conf. Ser. **86**, 012001 (2007).
2) J. M. Carr, P. G. Galiatsatos, J. D. Gorfinkiel, A. G. Harvey, M. A. Lysaght, D. Madden, Z. Masin, M. Plummer, and J. Tennyson, Eur. Phys. J. D **66**, 58 (2012).
3) P. G. Burke, *R-Matrix Theory of Atomic Collisions: Application to Atomic, Molecular and Optical Processes* (Springer, Heidelberg, 2011).
4) J. Tennyson, Phys. Rep. **491**, 29 (2010).
5) J. J. Munro, S. Harrison, M. M. Fujimoto, and J. Tennyson, J. Phys.: Conf. Ser. **388**, 012013 (2012).
6) C. J. Gillan, J. Tennyson, and P. G. Burke, in *Computational Methods for Electron–Molecule Collisions*, ed. F. A. Gianturco and W. M. Huo (Springer, New York, 1995) p. 239.
7) J. Tennyson, C. J. Noble, and P. G. Burke, Int. J. Quantum Chem. **29**, 1033 (1986).
8) J. Tennyson, J. Phys. B **20**, L375 (1987).
9) J. Tennyson and N. Chandra, Comput. Phys. Commun. **46**, 99 (1987).
10) L. A. Morgan, J. Tennyson, and C. J. Gillan, Comput. Phys. Commun. **114**, 120 (1998).
11) K. Pfingst, B. M. Nestmann, and S. D. Peyerimhoff, J. Phys. B **27**, 2283 (1994).
12) M. Hiyama and N. Kosugi, Phys. Scr. **T115**, 136 (2005).
13) M. Tashiro, J. Chem. Phys. **132**, 134306 (2010).
14) M. Hiyama and N. Kosugi, J. Theor. Comput. Chem. **4**, 35 (2005).
15) M. Tashiro, K. Ueda, and M. Ehara, Chem. Phys. Lett. **521**, 45 (2012).
16) A. G. Harvey, D. S. Brambila, F. Morales, and O. Smirnova, J. Phys. B **47**, 215005 (2014).
17) A. Rouzée, A. G. Harvey, F. Kelkensberg, D. Brambila, W. K. Siu, G. Gademann, O. Smirnova, and M. J. J. Vrakking, J. Phys. B **47**, 124017 (2014).
18) J. Tennyson, J. Phys. B **29**, 1817 (1996).
19) L. Tao, C. W. McCurdy, and T. N. Rescigno, Phys. Rev. A **79**, 012719 (2009).
20) P. V. Demekhin, A. Ehresmann, and V. L. Sukhorukov, J. Chem. Phys. **134**, 024113 (2011).
21) E. K. U. Gross and W. Kohn, in *Advances in Quantum Chemistry*, ed. P. O. Lwdin (Academic Press, New York, 1990) Density Functional Theory of Many-Fermion Systems, Vol. 21, p. 255.
22) M. Stener, D. Toffoli, G. Fronzoni, and P. Decleva, Theor. Chem. Acc. **117**, 943 (2007).
23) A. J. Krueger and N. T. Maitra, Phys. Chem. Chem. Phys. **11**, 4655 (2009).
24) D. L. Lynch and B. I. Schneider, Phys. Rev. A **45**, 4494 (1992).
25) A. E. Orel and T. N. Rescigno, Chem. Phys. Lett. **269**, 222 (1997).
26) R. R. Lucchese, K. Takatsuka, and V. McKoy, Phys. Rep. **131**, 147 (1986).
27) R. E. Stratmann, R. W. Zurales, and R. R. Lucchese, J. Chem. Phys. **104**, 8989 (1996).
28) E. D. Poliakoff and R. R. Lucchese, Phys. Scr. **74**, C71 (2006).
29) K. L. Baluja, C. J. Noble, and J. Tennyson, J. Phys. B **18**, L851 (1985).
30) B. I. Schneider and L. A. Collins, J. Phys. B **18**, L857 (1985).
31) M. A. P. Lima, T. L. Gibson, W. M. Huo, and V. McKoy, J. Phys. B **18**, L865 (1985).
32) J. Jose, R. R. Lucchese, and T. N. Rescigno, J. Chem. Phys. **140**, 204305 (2014).
33) J. A. R. Samson, G. N. Haddad, and J. L. Gardner, J. Phys. B **10**, 1749 (1977).
34) N. Wainfan, W. C. Walker, and G. L. Weissler, Phys. Rev. **99**, 542 (1955).
35) C. Backx and M. J. Van der Wiel, J. Phys. B **8**, 3020 (1975).
36) M. J. van der Wiel, W. Stoll, A. Hamnett, and C. E. Brion, Chem. Phys. Lett. **37**, 240 (1976).
37) P. G. Burke and K. T. Taylor, J. Phys. B **8**, 2620 (1975).
38) P. G. Burke, in *Atomic and Molecular Collision Theory*, ed. F. A. Gianturco (Plenum, New York, 1982) p. 69.
39) B. K. Sarpal, S. E. Branchett, J. Tennyson, and L. A. Morgan, J. Phys. B **24**, 3685 (1991).
40) H. J. Werner, P. J. Knowles, G. Knizia, F. R. Manby, and M. Schütz, WIREs Comput. Mol. Sci. **2**, 242 (2012).
41) M. Lebech, J. C. Houver, G. Raseev, A. S. dos Santos, D. Dowek, and R. R. Lucchese, J. Chem. Phys. **136**, 094303 (2012).
42) J. Tennyson, J. Phys. B **29**, 6185 (1996).
43) A. Faure, J. D. Gorfinkiel, L. A. Morgan, and J. Tennyson, Comput. Phys. Commun. **144**, 224 (2002).
44) T. Trickl, E. F. Cromwell, Y. T. Lee, and A. H. Kung, J. Chem. Phys. **91**, 6006 (1989).
45) D. A. Little and J. Tennyson, J. Phys. B **46**, 145102 (2013).
46) D. A. Little and J. Tennyson, J. Phys. B **47**, 105204 (2014).
47) J. Berkowitz, J. P. Greene, H. Cho, and B. Rusci, J. Chem. Phys. **86**, 674 (1987).
48) A. Hamnett, W. Stoll, and C. Brion, J. Electron Spectrosc. Relat. Phenom. **8**, 367 (1976).